International Journal of Biological Macromolecules 186 (2021) 79–91

Contents lists available at ScienceDirect

International Journal of Biological Macromolecules

journal homepage: www.elsevier.com/locate/ijbiomac

Intelligent modeling and experimental study on methylene blue adsorption by sodium alginate-kaolin beads

Nader Marzban [a,b,*], Ahmad Moheb [b], Svitlana Filonenko [c], Seyyed Hossein Hosseini [d], Mohammad Javad Nouri [b], Judy A. Libra [a], Gianluigi Farru [e]

[a] Leibniz Institute of Agricultural Engineering and Bio-economy e.V. (ATB), Max-Eyth-Allee 100, 14469 Potsdam, Germany
[b] Department of Chemical Engineering, Isfahan University of Technology, Isfahan 8415683111, Iran
[c] Max Planck Institute of Colloids and Interfaces, Am Mühlenberg 1, 14476 Potsdam, Germany
[d] Department of Chemical Engineering, Ilam University, Ilam 69315−516, Iran
[e] Department of Civil and Environmental Engineering and Architecture, University of Cagliari, Via Marengo, 2, 09123 Cagliari, Italy

ARTICLE INFO

Keywords:
Methylene blue adsorption
Sodium alginate-kaolin beads
Intelligent approaches

ABSTRACT

As tighter regulations on color in discharges to water bodies are more widely implemented worldwide, the demand for reliable inexpensive technologies for dye removal grows. In this study, the removal of the basic dye, methylene blue, by adsorption onto low-cost sodium alginate-kaolin beads was investigated to determine the effect of operating parameters (initial dye concentration, contact time, pH, adsorbent dosage, temperature, agitation speed) on dye removal efficiency. The composite beads and individual components were characterized by a number of analytical techniques. Three models were developed to describe the adsorption as a function of the operating parameters using regression analysis, and two powerful intelligent modeling techniques, genetic programming and artificial neural network (ANN). The ANN model is best in predicting dye removal efficiency with $R^2 = 0.97$ and RMSE = 3.59. The developed model can be used as a useful tool to optimize treatment processes using the promising adsorbent, to eliminate basic dyes from aqueous solutions. Adsorption followed a pseudo-second order kinetics and was best described by the Freundlich isotherm. Encapsulating the kaolin powder in sodium alginate resulted in removal efficiency of 99.56% and a maximum adsorption capacity of 188.7 $mg.g^{-1}$, a more than fourfold increase over kaolin alone.

1. Introduction

Dye-containing wastewaters are discharged from various industries such as textile, paper and food processing, dyestuff production, as well as from medical laboratories and households. Many dyes are complex organic compounds with high solubility in water and poor biodegradability, thus they are difficult to remove with conventional treatment methods [1,2]. The discharge of dyes to the environment can be harmful to the health of ecosystems and humans through direct effects due to the uptake of cancerogenic/mutagenic dyes or their byproducts, or indirectly through aesthetic impact or interference with photosynthesis in the receiving aquatic ecosystems [3]. Existing guidelines and regulations for the discharge of colored wastewater from the textile industry limit the spectral absorption coefficient (SAC) at three wavelengths (436, 525, 620 nm) to 7, 5, 3 m^{-1}, respectively [4,5]. The recent voluntary standard by the global industry initiative Zero Discharge of Hazardous Chemicals Programme for discharges from the textile industry goes beyond regulatory compliance to ensure that the environment and surrounding communities are not adversely affected [6]. They propose reductions in the SAC down to 2; 1; 1 m^{-1}, respectively. For a common basic dye such as methylene blue, these restrictions require concentrations as low as 0.025 ppm to achieve a SAC (620 nm) of 1 m^{-1}. Methylene blue is often selected as a proxy for basic dyes in color removal studies. It can be found in wastewaters from the paper, silk, acrylics and cosmetics industries, as well as laboratory and medical procedures [7].

The move for tighter regulations on dye concentrations in wastewater discharges requires inexpensive reliable technology for color removal. Much research and development activity has been carried out over the last decades to decolorize wastewaters containing organic dyes using biological reactors and different oxidation or reduction techniques to transform the dyes, using membranes or adsorption processes to

* Corresponding author at: Leibniz Institute of Agricultural Engineering and Bio-economy e.V. (ATB), Max-Eyth-Allee 100, 14469 Potsdam, Germany.
E-mail address: nmarzban@atb-potsdam.de (N. Marzban).

https://doi.org/10.1016/j.ijbiomac.2021.07.006
Received 15 March 2021; Received in revised form 1 July 2021; Accepted 1 July 2021
Available online 5 July 2021

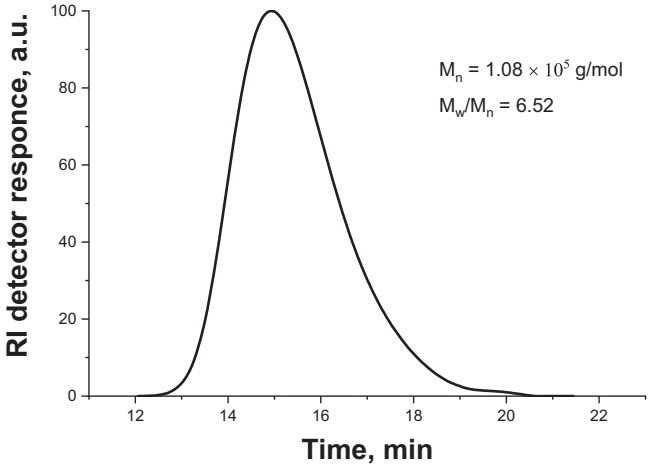

Fig. 1. GPC trace of sodium alginate.

Table 1
Characteristic parameters of the alginate calculated from the ^{1}H NMR spectra.

G	M	GG	MG	MM	GGM	MGM	GGG
0.92	0.95	0.56	0.64	0.31	0.44	0.20	0.12
FG	FM	FGG	FMG	FMM	FGGM	FMGM	FGGG
0.49	0.51	0.3	0.34	0.16	0.24	0.11	0.06

Table 2
Number average of block length is calculated as previously reported by Grasdalen [25].

NG	NG > 1	NM
1.44	1.58	1.5

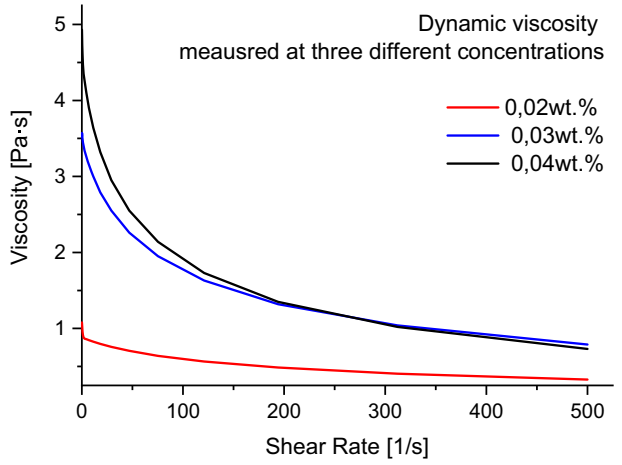

Fig. 2. Dynamic viscosity of the water solutions of alginate with three different concentrations.

remove the dyes [1,3,8,9].

Adsorption has been the focus of many studies since it does not produce metabolites [10,11]. Among the different types of adsorbents, activated carbon and carbon nanotube are widely studied for the removal of organic dye [12] and cationic heavy metals [13,14] due to their high adsorption capacity. However, the high costs and difficulties in the recovery process have raised interest in the use of cheaper and more efficient adsorbent materials, such as clays [10,12,15]. Kaolin as a type of clay is a promising adsorbent [16]; however, its application has

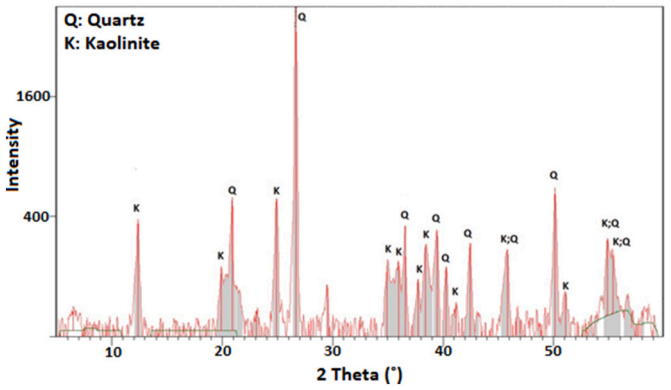

Fig. 3. XRD of kaolin powder.

Table 3
The six factors (operating parameters) used for the Box-Behnken design of experiment, the symbols used to represent them, and the coded and real values of each factor.

Factor	Symbol	Level		
–	–	−1	0	1
Temperature (°C)	A	20	27	34
Agitation speed (rpm)	B	100	145	190
Contact time (min)	C	20	70	120
Initial dye concentration (ppm)	D	4	18	32
pH of solution	E	3	6	9
Adsorbent dosage (g/L)	F	0.2	0.6	1

been restricted by the difficulties associated with its recovery from aqueous solution and low stability in fixed bed adsorption columns. Therefore, composites of powders such as kaolin with other materials that can facilitate their recovery and improve their applicability are being sought. Alginate is an inexpensive, nontoxic biopolymer that is known as an effective biosorbent due to the presence of carboxyl groups in its chains [17]. Sodium alginate has been shown to produce effective composite adsorbents with inorganic (zeolite/nickel ferrite) [18] and organic (rice husk) [19] components. Both composites were shown to be effective in the adsorption of methylene blue. Embedding clay in an alginate beads has a twofold benefit: the beads can be easily separated from the wastewater, while the rigid clay increases the mechanical resistance of the alginate [20].

Another important step in developing a low-cost adsorbent is being able to predict the required operating conditions for the desired dye removal. The initial dye concentration, contact time, pH value, adsorbent dosage, temperature and agitation speed can all play a role in determining the removal efficiency, and thus have to be predicted for efficient adsorption procedure. Regression models to describe the relationship between dye removal and many operating parameters can become quite complex and unwieldy to use [21]. In recent studies, researchers predicted the removal efficiency of dyes using artificial intelligence models like artificial neural network (ANN). Tanzifi et al. used a multilayer feed forward neural network to model the adsorption of methyl orange adsorption onto polyaniline nano-adsorbent [22]. In a similar study, the adsorption of Amido Black 10B on polyaniline/SiO2 nanocomposite was modeled using ANN [23]. Based on the good agreement between the experimental and predicted results, both studies concluded that the ANN model can be used to predict the removal efficiency of dyes. The form of ANN models is not explicit and hard to use. Another powerful tool, genetic programming (GP), an evolutionary computing technique based on a tree representation of genes [24], has been used to develop predictive models in industrial processing systems [25]. GP provides an explicit model to describe the relationship between the input and output variables.

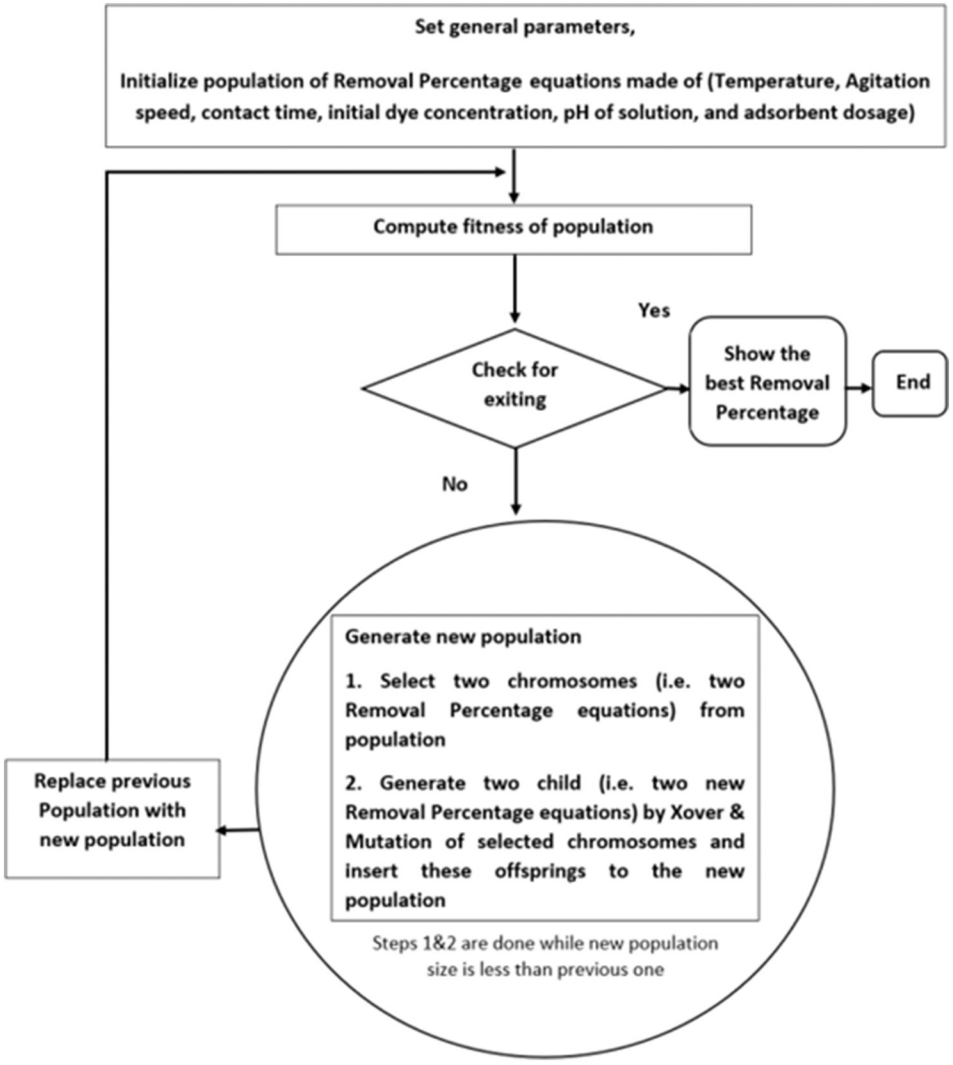

Fig. 4. Flowchart of the GP algorithm used to determine the model for methylene blue removal as a function of six operating parameters.

Table 4
Number of neurons and their corresponding RMSE and R^2.

Number. of neurons	Stage	Sample	RMSE	R^2
1	Training	36	7.21	0.87
	Validation	18	13.73	0.52
2	Training	36	6.27	0.90
	Validation	18	8.95	0.80
3	Training	36	6.20	0.91
	Validation	18	11.69	0.65
4	Training	36	4.14	0.95
	Validation	18	8.32	0.84
5	Training	36	2.90	0.98
	Validation	18	5.68	0.93
6	Training	36	6.87	0.88
	Validation	18	8.35	0.82
7	Training	36	7.61	0.86
	Validation	18	3.56	0.97
8	Training	36	6.10	0.91
	Validation	18	5.37	0.93
9	Training	36	3.63	0.97
	Validation	18	7.31	0.86
10	Training	36	3.77	0.96
	Validation	18	6.45	0.89
15	Training	36	7.91	0.84
	Validation	18	3.53	0.97
20	Training	36	9.85	0.76
	Validation	18	10.08	0.74

The purpose of the present work is to investigate the adsorptive properties of sodium alginate-kaolin beads in the removal of methylene blue from aqueous solution, in order to 1) determine equilibrium and kinetic adsorption models, 2) study how operating parameters affect dye removal efficiency, 3) develop a predictive model for the desired dye removal as a function of the operating conditions. The RSM Box-Behnken method was used to design the experiments to explore the effect of changes in the operating parameters (initial dye concentration, contact time, pH value, adsorbent dosage, temperature and agitation speed) on dye removal and to model the adsorption process. In addition, two powerful smart models of GP and ANN were used to model the adsorption of methylene blue on the beads. The outcomes of the three models were compared with the experimental data in order to choose the best model.

2. Materials and methods

2.1. Preparation and characterization of adsorbent

The sodium alginate was purchased from Acros Organics, USA with the reported purity of 19 to 25% (carboxyl groups) (on dried substance) and viscosity of 500 mPa·s for 1 wt% (20 °C) corresponding to average molecular weight of 100,000 g/mol. In addition, the molecular weight (MW = 108,000 g/mol) and number average were determined by the gel

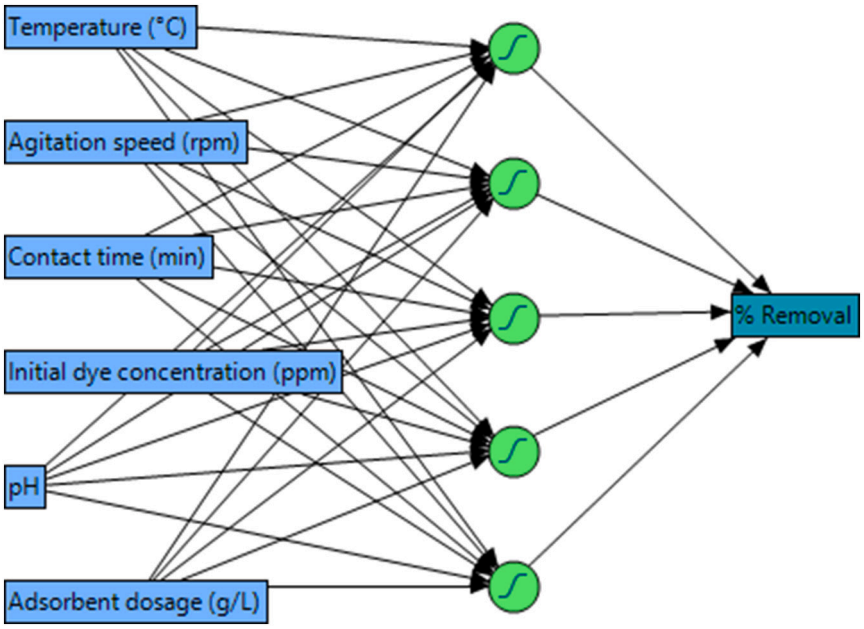

Fig. 5. Structure of neural network in the present study.

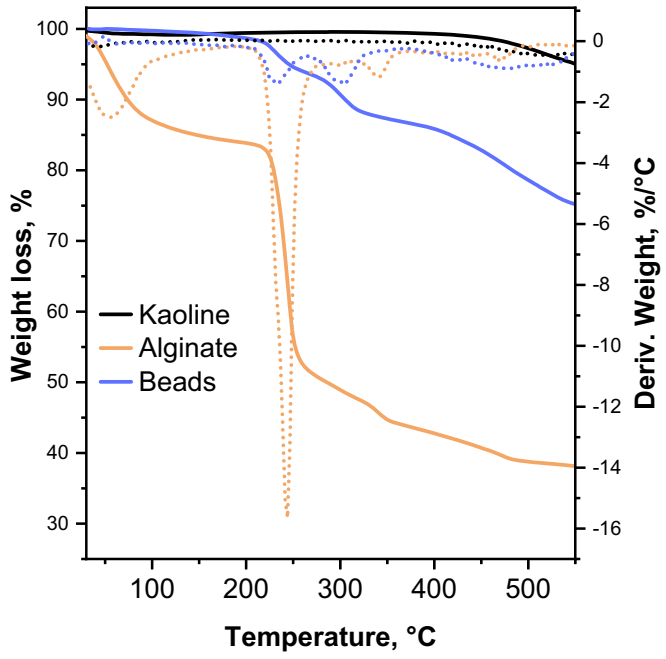

Fig. 6. Thermogravimetric analysis (TGA) of kaolin, alginate and alginate-kaolin beads performed under air atmosphere.

permeation chromatography (GPC) on PSS-SECurity-1260 Agilent GPC System equipped with PSS-SUPREMA-VS + HS-30 + HS-3000 Ä 10 μm column using Pullulan (PSS-Mainz) standards. The 0.1 N NaNO3 in double-distilled H2O was used as an eluent at a flow rate of 1.0 mL•min^{-1} at room temperature (Fig. 1).

The M/G ratio of alginate was determined by the ^{1}H NMR analysis following the standard procedure [26]. For this, alginate was hydrolyzed, and ^{1}H NMR spectrum was recorded with Varian 600 spectrometer at 80 °C. The characteristic parameters, such as mannuronate/guluronate (M/G) ratio, guluronic acid content (G-content), and average length of blocks of consecutive G monomer were calculated from the ^{1}H NMR spectrum (Tables 1 and 2).

The rheological properties of the alginate were determined on the Physica MCR 301; Anton Paar rotational rheometer (Fig. 2). The temperature was kept at 25 °C using a Peltier cooling module.

Kaolin was supplied by an Iranian industrial clay company. The kaolin powder was analyzed using X-Ray Diffraction (PMD Philips X-Pert, Netherlands) to identify the main compounds of the kaolin as quartz and kaolinite (Fig. 3).

Calcium chloride, sodium hydroxide, and hydrochloric acid, were purchased from Merck, Germany. Different kaolin to sodium alginate ratios (30:70, 40:60, 50:50, 60:40, 70:30, 80:20 and 75:25%) were used to synthesize the beads, and the goal was to use more kaolin in the beads. We should mention that the formed beads started to be fragmented at the percentage of more than 70% of kaolin. Therefore, the sodium alginate-kaolin beads were made by combining 70 wt% kaolin and 30 wt % sodium alginate powder. First, 1.4 g of kaolin powder was added to 100 mL of deionized water and stirred vigorously to uniformly disperse kaolin in water. In a second solution, 0.6 g of sodium alginate powder was added to 100 mL of deionized water and stirred. Both solutions were then mixed and stirred together for an hour. The resulting suspension was added drop-wise to 200 mL of a 0.5 M calcium chloride solution to form the alginate encapsulated kaolin beads. Since the size of the needle and the distance between needle and surface of calcium chloride film affect the shape and the diameter of produced beads [27], the distance was kept constant at 5 mm. Bead formation is caused by the development of cross-linkages in the alginate polymer chains due to the exchange of sodium for calcium cations [28].

$$\mathrm{Na\ (Alginate) + CaCl2 \rightarrow 2\ NaCl + Ca\ (Alginate)}$$

The beads were separated and washed with deionized water. To avoid the collapse of the internal structure, adsorbent beads were stored in deionized water until used.

Thermogravimetric investigation of pure kaolin and sodium alginate, and alginate-kaolin were carried out using a thermo microbalance TG 209 F1 Libra (Netzsch, Selb, Germany) on well ground samples in flowing air atmosphere. Each measurement was performed on 10 ± 1 mg of sample, which was placed in aluminium crucible and heated from 25 °C to 600 °C at a heating rate of 10 °C/min. Zeta potential measurements were carried out on a Zetasizer Nano ZS, Malvern Instruments (Malvern Panalytical, United Kingdom). The measured electrophoretic mobility was converted to Zeta potential using Smoluchowski's

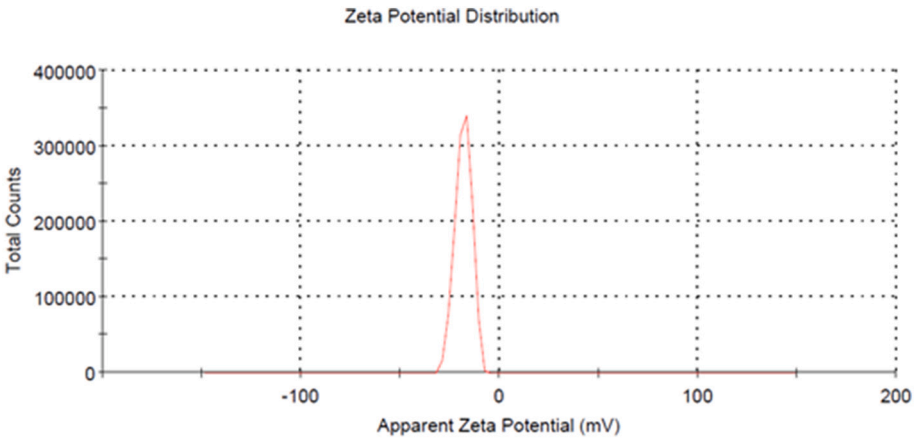

Fig. 7. Zeta potential of sodium alginate.

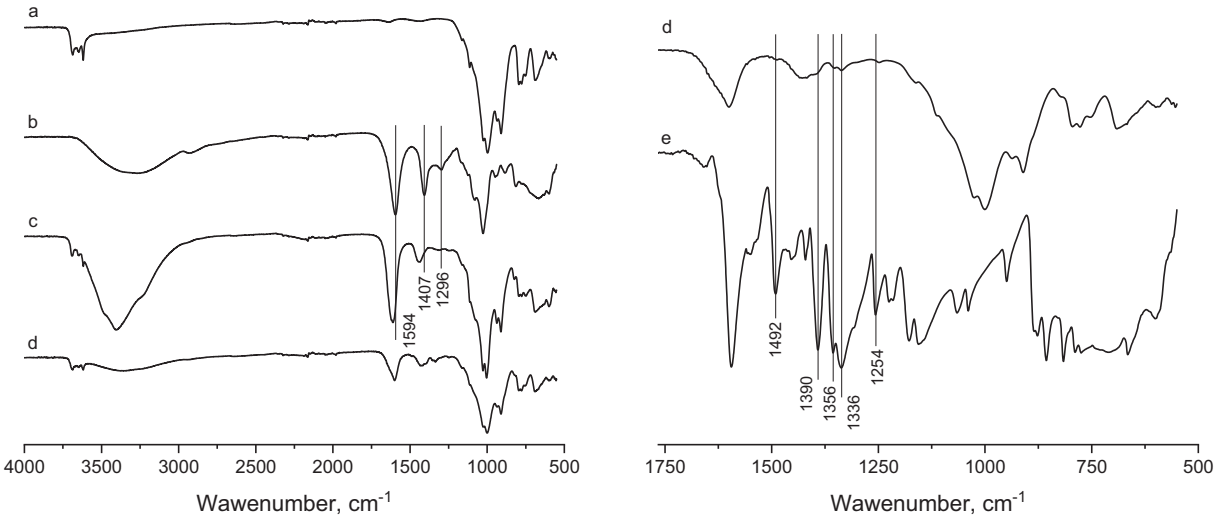

Fig. 8. FTIR - spectrum of: a) kaolin, b) sodium alginate, c) sodium alginate-kaolin beads before the adsorption, d) sodium alginate-kaolin beads after the adsorption, e) methylene blue.

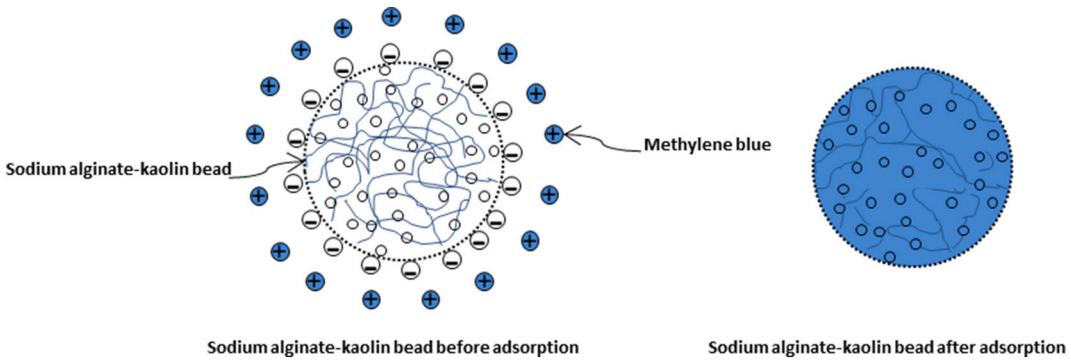

Fig. 9. Simple schematic of adsorption mechanism of methylene blue by sodium alginate-kaolin beads.

approximation. The samples for the measurement was prepared by stirring 30 mg of sodium alginate beads in 50 mL of bidistilled water for 12 h at room temperature. The obtained suspension was centrifuged for 3 min to precipitate the large particles and supernatant was measured for zeta potential. ATR-IR spectra of sodium alginate, kaolin and sodium alginate-kaolin beads before and after the adsorption were recorded on the Nicolet iS5 spectrometer from Thermo Fisher Scientific (Whaltham, Massachusettes, USA) equipped with iD5 ATR crystal. The spectra were recorded with a resolution of 0.5 cm-1. Furthermore, scanning electron microscopy (Phenom ProX Desktop SEM, USA) was used to study the surface morphology of sodium alginate, kaolin, and the sodium alginate-kaolin beads.

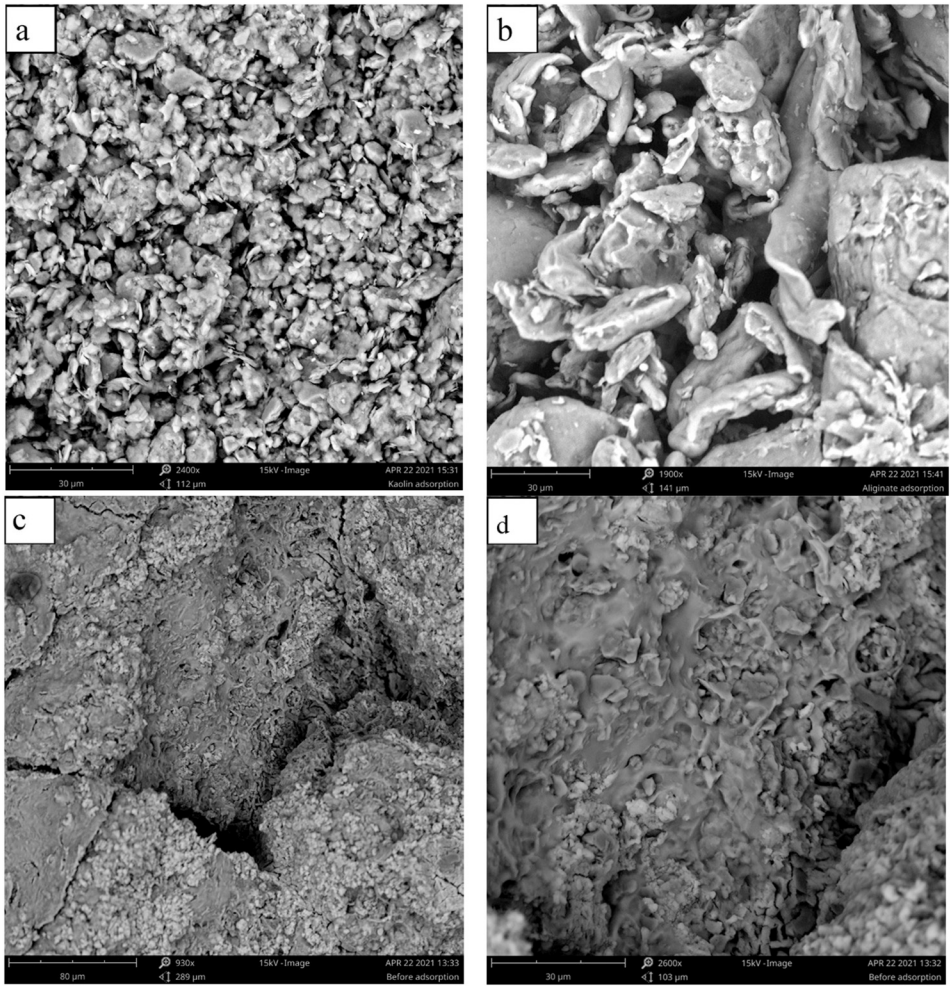

Fig. 10. SEM - images of sodium a) Kaolin, b) Sodium alginate, c and d) sodium alginate-kaolin beads.

Table 5
Regression model for the removal efficiency of methylene blue using 6 independent operational factors (A to F).

Regression model	R^2	Adjusted R^2	Root mean square error	Mean of responses	Observations
	0.87	0.81	8.76	76.33	54

%removal =

$$84.30 + 1.66\left(\frac{A-27}{7}\right) + 3.11\left(\frac{B-145}{45}\right) + 15.8\left(\frac{C-70}{50}\right) - 8.19\left(\frac{D-18}{14}\right) + 2.63\left(\frac{E-6}{3}\right) + 18.15\left(\frac{F-0.6}{0.4}\right) + 3.56\left(\frac{A-27}{7}\right)\left(\frac{B-145}{45}\right) - 3.72\left(\frac{B-145}{45}\right)\left(\frac{C-70}{50}\right) + 3.30\left(\frac{A-27}{7}\right)\left(\frac{D-18}{14}\right) + 4.49\left(\frac{A-27}{7}\right)\left(\frac{F-0.6}{0.4}\right) - 3.48\left(\frac{E-6}{3}\right)\left(\frac{F-0.6}{0.4}\right) - 6.6\left(\frac{A-27}{7}\right)^2 - 7.74\left(\frac{C-70}{50}\right)^2 + 6.70\left(\frac{D-18}{14}\right)^2 - 3.73\left(\frac{E-6}{3}\right)^2 - 6.55\left(\frac{F-0.6}{0.4}\right)^2$$

A: Temperature (°C); B: Agitation speed (rpm); C: Contact time (min); D: Initial dye concentration (mg L^{-1}); E: PH; F: Adsorbent dose (g/L).

2.2. Preparation of dye solutions

The basic dye methylene blue, a heterocyclic aromatic compound (MW = 319.85 g/mol, $C_{16}H_{18}ClN_3S$), was purchased from Uni-Chem Company. A stock solution of 1 g/L was prepared by dissolving 1 g of methylene blue in 1 L of deionized water and diluted with deionized water to achieve the specific concentrations required.

2.3. Adsorption studies

Adsorption experiments were designed using the response surface methodology in order to study the effects of the parameters such as temperature, agitation speed, time, initial dye concentration, pH value and adsorbent dosage. Based on preliminary experiments, three levels were chosen for the operating parameters: adsorbent dosage (0.2, 0.6 and 1 g·L^{-1}), initial dye concentration (4, 18 and 32 mg L^{-1}), agitation speed (100, 145 and 190 rpm), contact time (20, 70 and 120 min), solution temperature (20, 27 and 34 °C) and pH (3, 6 and 9). The pH was

Table 6
Analysis of variance and effect tests for removal of MB by sodium alginate-kaolin beads (* means the correlation term is statistically significant).

Source	DF	Sum of squares	F Ratio	Prob > F
Model	16	19,144.30	15.5882	<0.0001*
A: Temperature (°C)	1	65.97	0.8594	0.3599
B: Agitation speed (rpm)	1	232.32	3.0266	0.0902
C: Contact time (min)	1	5986.30	77.9893	<0.0001*
D: Initial dye concentration (ppm)	1	1609.83	20.9727	<0.0001*
E: pH of solution	1	165.74	2.1593	0.1502
F: Adsorbent dosage (g/L)	1	7908.68	103.0339	<0.0001*
Temperature (°C) × Agitation speed (rpm)	1	101.53	1.3227	0.2575
Agitation speed (rpm) × Contact time (min)	1	110.78	1.4433	0.2372
Temperature (°C) × Initial dye concentration (ppm)	1	174.90	2.2786	0.1397
Temperature (°C) × Adsorbent dosage (g/L)	1	161.01	2.0977	0.1559
pH of solution × Adsorbent dosage (g/L)	1	97.162	1.2658	0.2678
Temperature (°C) × Temperature (°C)	1	458.36	5.9715	0.0194*
Contact time (min) × Contact time (min)	1	628.76	8.1914	0.0069*
Initial dye concentration (ppm) × Initial dye concentration (ppm)	1	470.88	6.1346	0.0180*
pH of solution × pH of solution	1	155.72	2.0287	0.1627
Adsorbent dosage (g/L) × Adsorbent dosage (g/L)	1	451.11	5.8770	0.0203*
Lack of Fit	32	2633.32	1.9904	0.2279
Pure Error	5	206.73	–	–
Total Error	37	2840.05	–	–

adjusted by adding the proper amount of 0.1 M HCl and 0.1 M NaOH. The concentration of methylene blue in the solution was measured by a UV–Vis spectrophotometer (RAYLEIGH UV-2601 double beam, China) at the maximum adsorption wavelength (λ_{max} = 665 nm). Removal efficiency of methylene blue by sodium alginate-kaolin beads was determined using Eq. (1):

$$MB\ removal\ (\%) = \left(\frac{C_i - C_f}{C_i}\right) \times 100 \quad (1)$$

where C_i and C_f are the initial and final dye concentration (mg L^{-1}) in the solution, respectively.

2.4. Modeling and optimization

In this study, we used RSM, GP and ANN to predict the adsorption of MB on the beads. To evaluate the accuracy of the models, two metric errors were utilized. They are root mean squared error (RMSE) and coefficient of determination (R^2) that can be given by:

$$\mathrm{RMSE} = \sqrt{\frac{1}{n}\sum_{i=1}^{n}(X_c - X_e)^2} \quad (2)$$

where X_C is the calculated value by the model, X_e is the experimental value and n is the number of values.

$$R^2 = \left(1 - \frac{\sum_{i=1}^{n}(X_e - X_c)^2}{\sum_{i=1}^{n}\left(X_e - \overline{X_e}\right)^2}\right) \times 100 \quad (3)$$

where $\overline{X_e}$ is the average of experimental values.

2.4.1. Response surface methodology (RSM)

The Box-Behnken design of response surface methodology for 6 factors at 3 levels was selected in order to develop a second-order predictive equation. The experimental design was set up using JMP 14. The six operating parameters (temperature, agitation speed, contact time, initial dye concentration, pH and adsorbent dosage), their symbols used throughout the text (A-F) and the coded and real values for the three levels studied are listed in Table 3. A total number of 54 tests, including 6 central points, were designed. The experiments repeated twice (108 tests) and the average values were used to evaluate the removal efficiency (%) of methylene blue as the response (dependent variable).

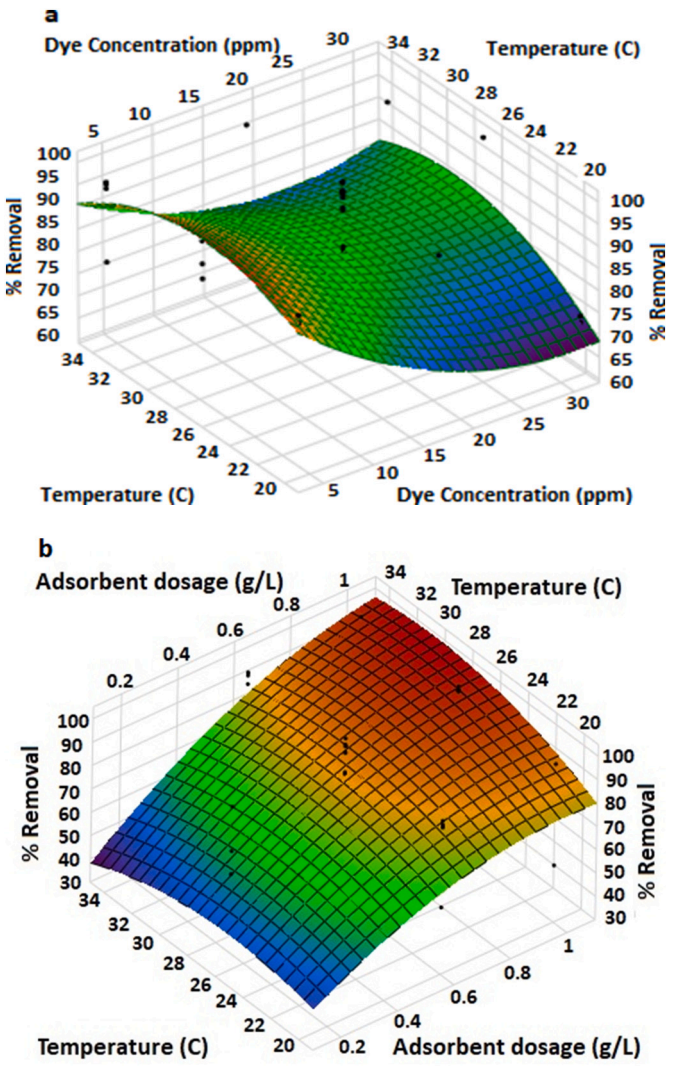

Fig. 11. Effect on MB removal efficiency by a) changes in initial dye concentration and temperature (agitation speed =145 rpm, contact time = 70 min, pH = 6, adsorbent dosage =0.6 g/L), b) changes in adsorbent dosages and temperature (agitation speed =145 rpm, contact time = 70 min, pH = 6, initial dye concentration = 18 ppm).

2.4.2. Genetic programming

In the present study, the GP was performed using eureqa toolbox [29] to develop predictive correlations based on temperature (°C), agitation speed (rpm), contact time (min), initial dye concentration (ppm), pH of solution and adsorbent dosage (g/L) as input variables and removal percentage as output. Fig. 4 shows the GP flowchart used in this research.

It contains the first population (i.e. initial population) that has several equations called individuals. By combining the selected individuals of the previous population, the next population is generated. The combination uses two main operations that are called crossover and mutation to manipulate individuals and generate the next individuals of the new generation (i.e. Crossover combines two selected individuals

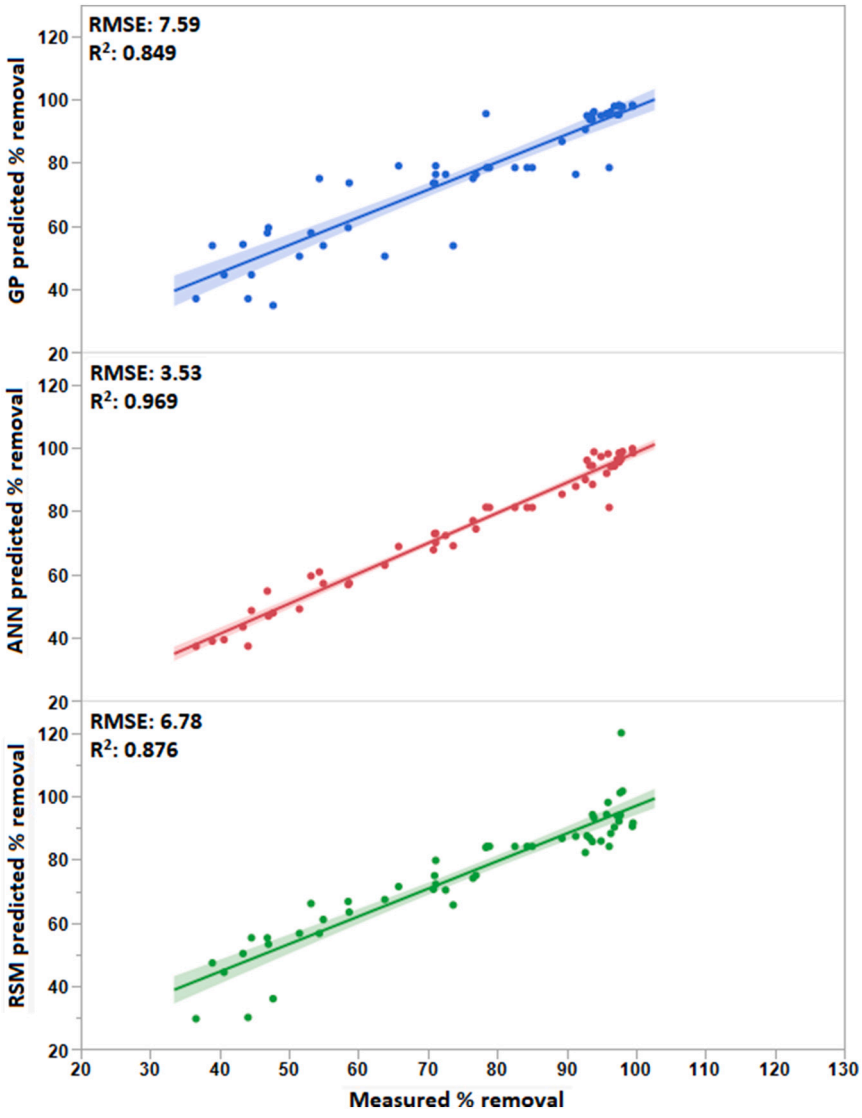

Fig. 12. Comparison between experimental data and those predicted by RSM, GP and ANN.

and the mutation works on the individuals generated by crossover). GP is stopped when one of the individuals of the next generation satisfies the criteria. More details about GP can be found elsewhere [25].

2.4.3. Artificial neural networks

In the last decade, the ANN models have been used to find the nonlinear relationship between input variables and removal efficiency of dye adsorption process [30]. The different layers of ANN models are considered as an input layer, one or more hidden layers and an output layer [31]. The ANN modeling was performed using JMP 14 to predict the adsorption efficiency of methylene blue. The training and validation sets are created by subsetting the data in two parts. The Holdback method with the proportion of 0.333 was used. Therefore, the data were randomly divided into 36 and 18 samples as training and validation subsets, respectively. Six neurons (Temperature (°C), agitation speed (rpm), Contact time (min), Initial dye concentration (ppm), pH of solution, and Adsorbent dosage (g/L)) were considered as input layer, one to twenty neurons in the hidden layer and one neuron (removal percentage) in the output layer were applied.

According to Table 4, the optimum number of neurons in the hidden layer, as 5 neurons, was chosen based on the minimum RMSE and maximum R^2. Fig. 5 shows the structure of neural network used in this study.

2.5. Adsorption kinetics

The adsorbed amount of MB was calculated in terms of mass of adsorbed material per unit mass of the adsorbent using the Eq. (4).

$$q_e = \frac{V(C_i - C_f)}{M} \tag{4}$$

where, C_f and C_i are the final equilibrium concentration and the initial concentration (mg L^{-1}), respectively, V is the volume of solution (L), and M denotes adsorbent weight (g).

In this study, the pseudo-first-order and pseudo-second-order kinetic models were used to investigate the dynamic behavior of the adsorption process [32]. The equation for the pseudo-first-order kinetic model is:

$$ln(q_e - q_t) = lnq_e - K_1 t \tag{5}$$

where q_e (mg g^{-1}) and q_t (mg g^{-1}) are the adsorption capacity at equilibrium and the adsorption capacity at an arbitrary time, t (min), respectively. K_1 (min^{-1}) is the pseudo-first-order constant rate.

The pseudo-second-order kinetic model is defined as:

$$\frac{t}{q_t} = \frac{1}{K_2 q_e^2} + \frac{t}{q_e} \tag{6}$$

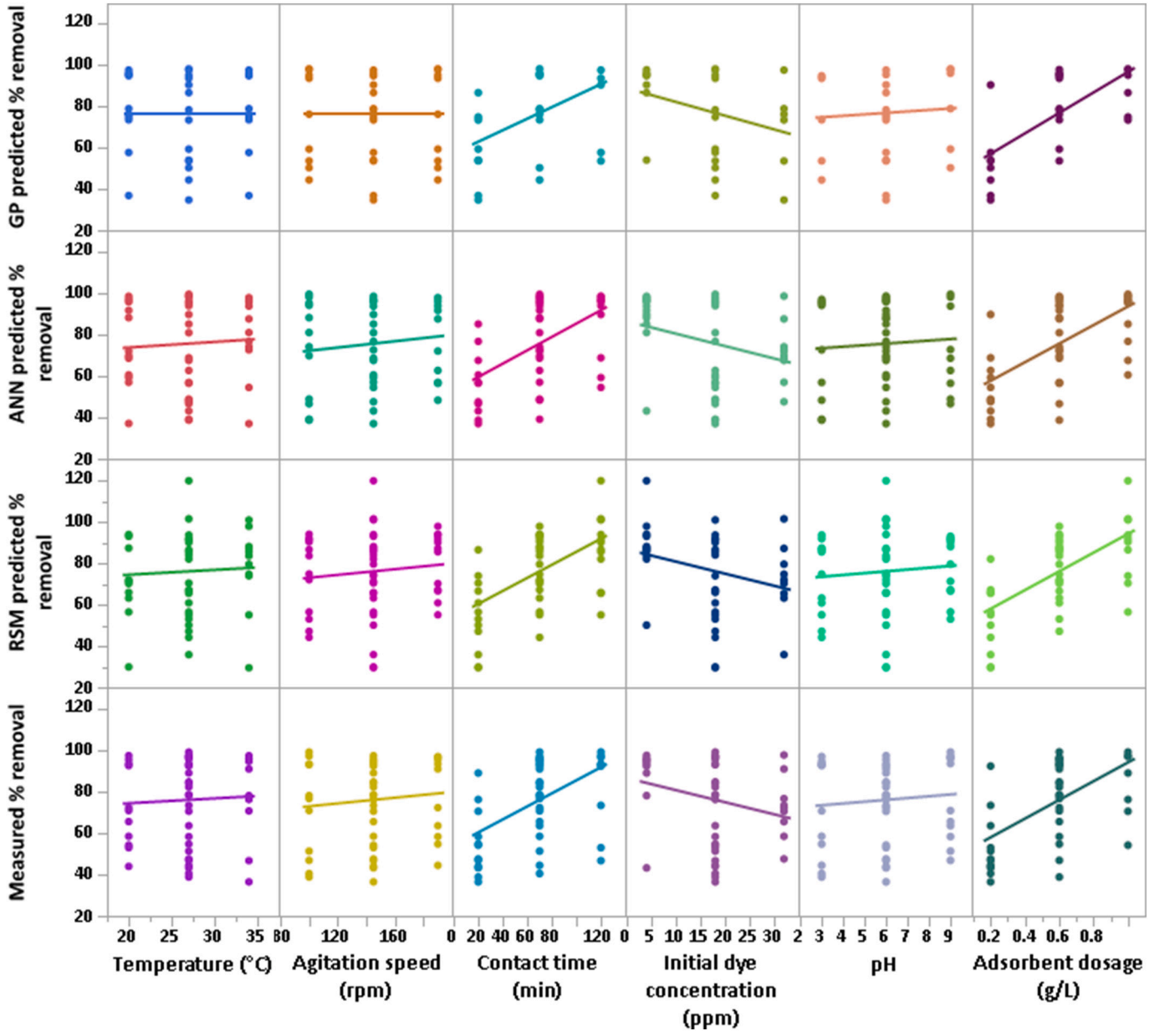

Fig. 13. Effect of operating conditions on %removal of MB.

Table 7
Sensitivity analysis of correlation offered by GP.

Variable	Sensitivity	% Positive	Positive magnitude	% Negative	Negative magnitude
Adsorbent dosage	0.58	100%	0.58	0%	0
Time	0.46	100%	0.46	0%	0
Initial dye concentration	0.26	0%	0	100%	0.26
pH	0.055	100%	0.055	0%	0

where K_2 (min^{-1}) is the pseudo-second-order constant rate.

2.6. Adsorption isotherms

Three widely used isotherm models of Langmuir, Freundlich, and Temkin were employed to study the adsorption mechanism [32,35,36]. The linear form of the models was used (Eqs. (7) to (9)). Langmuir isotherm model:

$$\frac{C_e}{q_e} = \frac{C_e}{q_m} + \frac{1}{K_L q_m} \quad (7)$$

where q_e (mg g^{-1}) is the amount of dye adsorbed on the adsorbent at equilibrium, q_m (mg g^{-1}) is the maximum adsorption capacity, K_L is the equilibrium constant and C_e (mg L^{-1}) is dye concentration at equilibrium. Freundlich isotherm:

Table 8
Summary of correlations.

Model	Correlation
RSM	$\%\ \text{Removal} = 84.30 + 1.66\left(\frac{\text{Temperature}-27}{7}\right) + 3.11\left(\frac{\text{Agitation speed}-145}{45}\right) + 15.8\left(\frac{\text{Contact time (min)}-70}{50}\right) - 8.19\left(\frac{\text{Initial dye concentration}-18}{14}\right) + 2.63\left(\frac{\text{pH}-6}{3}\right) + 18.15\left(\frac{\text{Adsorbent dose}-0.6}{0.4}\right) + 3.56\left(\frac{\text{Temperature}-27}{7}\right)\left(\frac{\text{Agitation speed}-145}{45}\right) - 3.72\left(\frac{\text{Agitation speed}-145}{45}\right)\left(\frac{\text{Contact time}-70}{50}\right) + 3.30\left(\frac{\text{Temperature}-27}{7}\right)\left(\frac{\text{Initial dye concentration}-18}{14}\right) + 4.49\left(\frac{\text{Temperature}-27}{7}\right)\left(\frac{\text{Adsorbent dose}-0.6}{0.4}\right) - 3.48\left(\frac{\text{pH}-6}{3}\right)\left(\frac{\text{Adsorbent dose}-0.6}{0.4}\right) - 6.6\left(\frac{\text{Temperature}-27}{7}\right)^2 - 7.74\left(\frac{\text{Contact time}-70}{50}\right)^2 + 6.70\left(\frac{\text{Initial dye concentration}-18}{14}\right)^2 - 3.73\left(\frac{\text{pH}-6}{3}\right)^2 - 6.55\left(\frac{\text{Adsorbent dose}-0.6}{0.4}\right)^2$
GP	$\%\ \text{Removal} = 15.71 + \text{pH} + (34.75 \times \text{Adsorbent dosage}) + (0.8439 \times \text{time} \times \text{adsorbent dosage}) + (72.4 + \text{time} - 0.8439 \times \text{time} \times \text{adsorbent dosage}) - \left(\frac{0.1257 \times \text{time} \times \text{pH} \times \text{Adsorbent dosage}^2}{\text{Initial dye concentration}}\right) - (0.004167 \times \text{time}^2 \times \text{adsorbent dosage}^3)$
ANN	Reported in Table 2S of Supplementary material

Temperature (°C); Agitation speed (rpm); Contact time (min); Initial dye concentration (mg L^{-1}); pH; Adsorbent dose (g/L).

Table 9
Kinetics parameters for adsorption of MB by sodium alginate-kaolin beads.

Initial dye concentration (mg·L^{-1})	$q_{e,expt}$ (mg·g^{-1})	Pseudo-first-order kinetic			Pseudo-second-order kinetic		
		$q_{e,cal}$ (mg·g^{-1})	K_1 (min^{-1})	R^2	$q_{e,cal}$ (mg·g^{-1})	K_2 (g·mg^{-1} min^{-1})	R^2
12	11.57	3.46	0.04	0.98	11.60	0.01	0.992

Table 10
Isotherm parameters for adsorption of MB by sodium alginate-kaolin beads.

Isotherm	Parameter	Values
Langmuir	q_m (mg·g^{-1})	188.67
	K_L (L·mg^{-1})	0.046
	R^2	0.88
Freundlich	KF	10.29
	n	1.28
	R^2	0.992
Temkin	B	89.174
	K_T (L mol^{-1})	0.0143
	R^2	0.91
	b_T	25.46

$$\text{Ln}\ q_e = \text{Ln}\ k_F + \frac{1}{n}\text{Ln}\ C_e \quad (8)$$

where k_F and n are Freundlich constants related to the adsorption capacity and its intensity, respectively. Temkin isotherm:

$$q_e = \text{BLn}K_T + \text{BLn}C_e \quad (9)$$

where B = RT/b_T, K_T (L mol^{-1}) is the equilibrium constant with maximum graft energy. R (8.314 J mol^{-1} K^{-1}) is the gas constant, T (K) is the absolute temperature, and b_T(J mol^{-1}) is the constant for the nature of the adsorption energy.

3. Results and discussions

3.1. Adsorbent characterization

The sodium alginate-kaolin beads and their individual components were subjected to various analytical methods to better understand their structure. Comparative thermogravimetric analysis performed on the

Table 11
The maximum adsorption capacity values of different adsorbents for MB removal from aqueous solutions.

Ref	Maximum adsorption capacities(mg g^{-1})	Adsorbent	
[45]	756.97	Calcium alginate–bentonite–activate carbon composite bead	Composite
[19]	274.9	Magnetic alginate/rice husk bio-composite	
This study	188.67	Sodium alginate-kaolin beads	
[47]	180.32	Cellulose/carboxylated graphene oxide composite microbeads	
[48]	90.7	Polydopamine microspheres	
[16]	54.05	Zeolite/nickel ferrite/sodium alginateBionanocomposite	
[49]	20.55	Seaweed-ZnO-PANI hybrid composite	
[16]	45	Kaolin	Powder
[46]	13.99	Raw kaolin	
[46]	20.49	NaOH-treated pure kaolin	

pristine materials and prepared beads (Fig. 6) reveals strong interaction of the alginate with the kaolin carrier. Namely, pure kaolin shows in the TGA ca. 7% mass loss, which occurred at temperatures above 400 °C and can be attributed to the loss of interstitial water [37]. The thermal decomposition of pure alginate is in agreement with the literature [38], with considerable water loss at temperatures below 100 °C (13% mass loss), and intensive weight loss at 240 °C indicating the rupture of the alginate structure, destruction of chains into monomers and fragments, loosing up to 50% of mass. Further gradual mass loss at higher temperatures is related to the decomposition of the generated fragments. The thermal behavior of the alginate-kaolin beads is qualitatively and quantitatively different from the pure components. Water loss at temperatures below 100 °C is not pronounced in the composite. The large mass loss (7% in accordance with the composition of the beads where the content of alginate reach 30 wt%) that corresponds to the alginate degradation occurs at slightly lower temperature (235 °C), though a second mass loss of almost same value occurs at 300 °C. This could point to stabilization of the alginate bonded to kaolin.

The sodium alginate beads have a neat negative charge of average value −18.2 mV. Fig. 7 shows the zeta potential measurement graph obtained for sodium alginate dispersed in water.

The vibrational spectroscopy was performed on pristine materials and prepared beads before and after the adsorption in order to evaluate the interaction of alginate with kaolin upon formation of the beads and to determine functional groups responsible for adsorption of methylene blue (Fig. 8). On the FT-IR spectrum of pristine kaolin, vibrational modes at 682 cm^{-1} and 909 cm^{-1} correspond to Al-OH vibrations, the Si-O-Al groups appeared at 588 cm^{-1} and 780 cm^{-1}. The bands at 996 cm^{-1} and 1115 cm^{-1} are characteristic of Si—O bond. The bands between 3618 and 3695 cm^{-1} are attributed to the OH stretching mode [39]. On the spectra of sodium alginate, the absorption bands of the hydroxyl group appeared between 3000 and 3600 cm^{-1}, aliphatic C—H was observed at 2929 cm^{-1} and the asymmetric and symmetric stretching vibrations of the carboxyl group were observed at 1594 and 1407 cm^{-1}, correspondingly. The band at 1296 cm^{-1} corresponds to stretching vibrations of the C-OH bond [40]. On the spectra of the beads (Fig. 8c) vibrational modes of kaolin [43] and alginate overlap, though a considerable shift of the vibrational modes of alginate is observed. Namely higher vibrational frequency of hydroxyl groups appearing at 3420 cm^{-1} due to the weakening of the strength of the O—H bond when involved in hydrogen bonding [41]. The frequencies of stretching vibrations in carboxyl groups are occur at 1610 and 1437 cm^{-1} comparatively to pristine alginate. The high wavenumbers shift indicates involvement of the OH and COOH groups of alginate in hydrogen bonding to the hydroxil groups of kaolin. On the FTIR spectra of the beads after the adsorption, vibrational modes of methylene blue are clearly distinguishable: bands at 1492 cm^{-1} (ν_{het}(C—C)), 1390 cm^{-1} (ν_{het}(C═S^{+})), 1356 cm^{-1} (δ_{as}(CH), δ_{s}(CH)), 1336 cm^{-1} (ν(C—N) in N-CH_3)), 1254 cm^{-1} (δ(CH), γ(C—H)) [42] of the methylene blue dye appear. Simultaneously the vibrational modes of OH and COOH groups of alginate shift to the lower wavelengths. This behavior might reveal the weakening of the interaction of alginate with kaolin due to the competitive interaction with the dye molecules via hydroxyl and carboxyl groups [33,34].

A simple adsorption mechanism is shown in Fig. 9. The negative charge of the beads is responsible for the adsorption of the cationic dye, methylene blue.

The sodium alginate-kaolin beads were analyzed by scanning electron microscopy (SEM), which gives an overview of surface morphology. The SEM images (Fig. 10), of kaolin, sodium alginate, and sodium alginate-kaolin beads, show the uniform surface coating of kaolin by alginate without the separate phase of alginate particles which result in a homogeneous structure of the beads. This implies that the synthesized adsorbents have a significant surface which are corresponding to initial surface of kaolin available for the adsorption of methylene blue.

3.2. Statistical analysis of the effect of the operational parameters on removal efficiency

The dye removal was found to vary depending on the operational parameters. Values ranging from 36.59 to the maximum dye removal of 99.56% were achieved. (All results can be found in Table 1S in supplementary materials.) The relationship between the removal efficiency of MB and the 6 independent operational factors (A to F) was first analyzed within the framework of RSM. A regression equation was obtained by fitting the experimental data obtained from the Box-Behnken design with a second-order polynomial equation (Table 5). The R^2 of 0.87 shows reasonable agreement between the model and the data.

An ANOVA was conducted to study the effects and importance of the factors in the RSM regression model. The results are summarized in Table 5. The value of the F Ratio for the model of 15.5882 shows that the model is significant, while the lack-of-fit is not significant so that the model adequately explains data. The *p*-values for three of the six factors and their quadratic terms are less than 0.05 and indicate that these factors, C- contact time, D- initial dye concentration and F- adsorbent dosage, are significant. None of the terms for interaction among process parameters were significant. In addition, the terms with *P*-values of over 0.44 were removed and not reported in Table 6 to reduce and improve the model.

The response surface plot showing the effects of temperature and initial dye concentration on MB removal efficiency is shown in Fig. 11a. The other four factors were held constant at their central values (agitation speed =145 rpm, contact time = 70 min, pH = 6, adsorbent dosage = 0.6 g/L). Removal efficiency was highest at 27 °C for most the initial dye concentrations. Temperature increases from 20° to 34 °C had only a small effect on removal efficiency, as already seen from the regression analysis. This may be an important characteristic since the temperature of dye-containing wastewaters can vary widely. In contrast, by increasing the initial dye concentration, the dye removal efficiency was decreased. Increasing the initial dye concentration from 4 to 18 ppm at 20 °C, decreased the removal efficiency from 90 to 75%. However, further increases to 32 ppm showed little effect. Increasing the adsorbent dosage from 0.2 to 0.6 g/L, raised removal efficiency from 40 to 80% (Fig. 11b). The temperature had only a slight effect on the dye removal at the different adsorbent dosages.

3.3. Comparison of models

The RSM regression model developed in the previous section can be used to predict the removal efficiency as a function of the operating conditions. However, trials were made with other powerful modeling techniques, GP and ANN, to see whether less complex models are possible. The accuracy of RSM, ANN and GP for prediction of removal efficiency are compared in Fig. 12. The ANN with relatively good values of R^2 of 0.97 and RMSE of 3.53 is the most appropriate method for prediction of MB removal (Table 2S in supplementary materials). However, the correlation offered by ANN is very complex to be used for future prediction.

The effect of parameters such as temperature, agitation speed, contact time, initial dye concentration, pH of the solution and adsorbent dosage on dye removal is shown in Fig. 13. The contact time showed a significant effect on measured and predicted dye removal, and by increasing the contact time, dye removal was constantly increased until the experimental time of 120 min. Moreover, dye removal was reduced by increasing the initial dye concentration. The pH of the solution had the smallest effect on the adsorption process, and increasing the pH was in favor of the adsorption process. The adsorbent dosage shows the most significant enhancing effect, over 30%, on the dye removal process.

Fig. 13 also shows that the temperature and agitation speed have no influence on predicted % removal using GP. Table 7 shows sensitivity analysis of the GP model. The % positive is the likelihood that increasing this variable will increase the MB removal variable. Therefore, the

increase in adsorbent dosage, contact time and pH leads to increases in the MB removal. The comparison of the positive magnitude of these variables shows that the adsorbent dosage has the most significant effect on the methylene blue removal.

The initial dye concentration has a 100% negative effect and increase of this variable leads to a decrease in the removal efficiency. In contrast to ANN, the GP offers an explicit correlation which can be used for prediction of MB. Table 8 shows the correlations offered by different models. The ANN model correlation is reported in Table 2S of supplementary material. To use this correlation for prediction of %removal, the Model NTanH(5) need to be copied and paste into the JMP software as column properties.

One advantage of GP over RSM is the automatic removal of unimportant variables in the final correlation. This process must be manually performed in RSM correlations by comparing the *p*-value of each element in the correlation. From the experimental data, the optimized operating conditions offering the highest measured MB removal (99.56%) are $T = 27$ °C, agitation speed of 100 rpm, time of 120 min, initial dye concentration of 18 ppm, pH of 9, adsorbent dosage of 0.6 g. However, under these conditions the RSM, ANN and GP under predicted the removal efficiency as 91.66%, 98.52% and 97.96% respectively. It can be concluded that under most of the operating conditions, the ANN shows the better agreement with experimental data compared to GP and RSM models for prediction of MB adsorption by sodium alginate-kaolin beads. In a similar study, Tanzifi et al. [44] modeled the adsorption of Congo Red using RSM, GP and ANN and reported that the ANN offered the closest agreement with measured values.

3.4. Adsorption kinetics study

The experimental data was analyzed using Eqs. (5) and (6) to determine the kinetics of the adsorption. The corresponding kinetics parameters are reported in Table 9. The higher correlation coefficient of $R^2 = 0.99$ for the pseudo-second-order kinetic model and the very close values for $q_{e,expt}$ and $q_{e,cal}$ of the pseudo-second order model suggest that the chemical adsorption was limiting stage of the adsorption process.

3.5. Adsorption isotherms study

The experimental isotherm results were compared to three adsorption isotherm models, Langmuir, Freundlich and Temkin (Table 10). The parameters obtained from the linear curve fitting of the three adsorption models to the experimental data show that the adsorption process is best modeled with the Freundlich isotherm model, which indicates the adsorption process of methylene blue was via forming multi-layers of adsorbed molecules influenced by the non-uniform surface of the beads.

The maximum adsorption capacity determined by the Langmuir isotherm model was found equal to 188.67 mg g^{-1}. This value is compared in Table 11 to literature values for the adsorption capacities of methylene blue by various adsorbents. While two complex composites, the calcium alginate–bentonite–activate carbon composite bead [45] and magnetic alginate/rice husk bio-composite [19], had significantly higher adsorption capacities compared to the adsorbent used in our study, the simple to prepare sodium alginate-kaolin beads have a relatively high adsorption capacity compared to the other composite adsorbents. Encapsulating the kaolin powder in sodium alginate beads increased the adsorption capacity by over a factor of four higher than that measured for kaolin alone [16], [46].

4. Conclusions

Sodium alginate-kaolin beads were shown to be effective for the removal of methylene blue from aqueous solutions. The kinetic and isotherm studies showed that the adsorption of MB by the adsorbent used in this work followed the pseudo-second-order kinetic and Freundlich isotherm models, respectively, both with consistency coefficient of $R^2 > 0.99$. A relatively high value for the maximum adsorption capacity of the adsorbent was found, 188.67 mg g^{-1} at 27 °C, by implementing the Langmuir isotherm model. Dye removal efficiencies of almost 100% were found in the investigation of six operating parameters at three levels by the Box-Behnken method. The statistical analysis of the results showed that two parameters, contact time and adsorbent dosage, had the most influence on the adsorption properties of the adsorbent. The adsorptive capacity of the beads was relatively independent of pH, agitation speed and temperature, so that the adsorbent functioned well over a wide range of values likely to be found in dye-containing wastewaters and equipment. The results of modeling revealed that ANN is the best model to predict the removal efficiency of MB. It can be used to determine the operating conditions necessary to achieve a desired removal efficiency. Finally, the synthesized adsorbent was found to be a promising tool for removal of methylene blue from aqueous solutions.

Authorship statement

All persons who meet authorship criteria are listed as authors, and all authors certify that they have participated sufficiently in the work to take public responsibility for the content, including participation in the concept, design, analysis, writing, or revision of the manuscript. Furthermore, each author certifies that this material or similar material has not been and will not be submitted to or published in any other publication before its appearance in the International Journal of Biological Macromolecules.

Authorship contributions

Category 1

Conception and design of study: Nader Marzban, Ahmad Moheb, Seyyed Hossein Hosseini; **Acquisition of data:** Nader Marzban, Mohammad Javad Nouri, Gianluigi Farru; Svitlana Filonenko; **analysis and/or interpretation of data:** Nader Marzban, Svitlana Filonenko, Ahmad Moheb, Seyyed Hossein Hosseini, Judy A Libra.

Category 2

Drafting the manuscript: Nader Marzban, Ahmad Moheb, Judy A Libra; **revising the manuscript critically for important intellectual content:** Svitlana Filonenko, Nader Marzban, Ahmad Moheb, Judy A Libra, Seyyed Hossein Hosseini.

Category 3

Approval of the version of the manuscript to be published (the names of all authors must be listed): Nader Marzban, Ahmad Moheb, Svitlana Filonenko, Seyyed Hossein Hosseini, Mohammad Javad Nouri, Judy A Libra, Gianluigi Farru.

Acknowledgements All persons who have made substantial contributions to the work reported in the manuscript (e.g., technical help, writing and editing assistance, general support), but who do not meet the criteria for authorship, are named in the Acknowledgements and have given us their written permission to be named. If we have not included an Acknowledgements, then that indicates that we have not received substantial contributions from non-authors.

Acknowledgments

We thank Dr. Hans-Jörg Gusovius (Leibniz Institute of Agricultural Engineering and Bioeconomy) for providing SEM analysis, and Giovanna Rehde (Leibniz Institute of Agricultural Engineering and Bioeconomy) for providing chemicals and analytical techniques.

Appendix A. Supplementary data

Supplementary data to this article can be found online at https://doi.org/10.1016/j.ijbiomac.2021.07.006.

References

[1] O.J. Hao, H. Kim, P.-C. Chiang, Decolorization of wastewater, Crit. Rev. Environ. Sci. Technol. 30 (2000) 449–505, https://doi.org/10.1080/10643380091184237.

[2] V. Pande, S. Pandey, T. Joshi, D. Sati, S. Gangola, S. Kumar, M. Samant, in: Biodegradation of Toxic Dyes: A Comparative Study of Enzyme Action in a Microbial System, 2019, pp. 255–287, https://doi.org/10.1016/B978-0-12-818307-6.00014-7.

[3] ntegrated Pollution Prevention and Control (IPPC), Reference Document on Best Available Techniques for the Textiles Industry, 2003. https://eippcb.jrc.ec.europa.eu/sites/default/files/2019-11/txt_bref_0703.pdf. (Accessed 17 February 2021).

[4] German Ordinance on Requirements for the Discharge of Waste Water into Waters (Waste Water Ordinance – AbwV, Annex 38). https://www.gesetze-im-internet.de/abwv/anhang_38.html, 2004. (Accessed 17 February 2021).

[5] IFC-EHS Guidelines, Environmental, Health, and Safety General Guidelines for Textile Manufacturing, 2007. www.ifc.org/ehsguidelines. (Accessed 17 February 2021).

[6] ZDHC, Wastewater Guidelines Version 1.1, 2019. https://www.roadmaptozero.com/post/updated-zdhc-wastewater-guidelines-v1-1-released?locale=en. (Accessed 17 February 2021).

[7] PubChem, Methylene blue. https://pubchem.ncbi.nlm.nih.gov/compound/6099, 2021. (Accessed 17 February 2021).

[8] L. Bilinska, M. Gmurek, S. Ledakowicz, Comparison between industrial and simulated textile wastewater treatment by AOPs – biodegradability, toxicity and cost assessment, Chem. Eng. J. 306 (2016) 550–559, https://doi.org/10.1016/j.cej.2016.07.100.

[9] E.M.A. El-Monaem, M.M.A. El-Latif, A.S. Eltaweil, G.M. El-Subruiti, Cobalt nanoparticles supported on reduced amine-functionalized graphene oxide for catalytic reduction of nitroanilines and organic dyes, Nano 16 (2021) 2150039, https://doi.org/10.1142/S1793292021500399.

[10] M.Shahadat Momina, S. Isamil, Regeneration performance of clay-based adsorbents for the removal of industrial dyes: a review, RSC Adv. 8 (2018) 24571–24587, https://doi.org/10.1039/C8RA04290J.

[11] A.S. Eltaweil, A.M. El-Tawil, E.M. Abd El-Monaem, G.M. El-Subruiti, Zero valent iron nanoparticle-loaded nanobentonite intercalated carboxymethyl chitosan for efficient removal of both anionic and cationic dyes, ACS Omega 6 (2021) 6348–6360, https://doi.org/10.1021/acsomega.0c06251.

[12] A. Dincer, Y. Gunes, N. Karakaya, E. Gunes, Comparison of activated carbon and bottom ash for removal of reactive dye from aqueous solution, Bioresour. Technol. 98 (2007) 834–839, https://doi.org/10.1016/j.biortech.2006.03.009.

[13] B. Hayati, A. Maleki, F. Najafi, F. Gharibi, G. McKay, V.K. Gupta, S. Harikaranahalli Puttaiah, N. Marzban, Heavy metal adsorption using PAMAM/CNT nanocomposite from aqueous solution in batch and continuous fixed bed systems, Chem. Eng. J. 346 (2018) 258–270, https://doi.org/10.1016/j.cej.2018.03.172.

[14] B. Hayati, A. Maleki, F. Najafi, R. Rezaee, H. Puttaiah, N. Marzban, G. McKay, PPI/CNT nanocomposite for novel high capacity removal of the toxic heavy metals Hg, Pb and Ni from water, Desalin. Water Treat. 198 (2020) 190–199, https://doi.org/10.5004/dwt.2020.26079.

[15] B. Nandi, A. Goswami, M. Purkait, Removal of cationic dyes from aqueous solutions by kaolin: kinetic and equilibrium studies, Appl. Clay Sci. 42 (2009) 583–590, https://doi.org/10.1016/j.clay.2008.03.015.

[16] K. Rida, S. Bouraoui, S. Hadnine, Adsorption of methylene blue from aqueous solution by kaolin and zeolite, Appl. Clay Sci. 83–84 (2013) 99–105, https://doi.org/10.1016/j.clay.2013.08.015.

[17] A. Ikeda, A. Takemura, H. Ono, Preparation of low-molecular weight alginic acid by acid hydrolysis, Carbohydr. Polym. 42 (2000) 421–425, https://doi.org/10.1016/S0144-8617(99)00183-6.

[18] M. Bayat, V. Javanbakht, J. Esmaili, Synthesis of zeolite/nickel ferrite/sodium alginate bionanocomposite via a co-precipitation technique for efficient removal of water-soluble methylene blue dye, Int. J. Biol. Macromol. 116 (2018) 607–619, https://doi.org/10.1016/j.ijbiomac.2018.05.012.

[19] E. Alver, A.Ü. Metin, F. Brouers, Methylene blue adsorption on magnetic alginate/rice husk bio-composite, Int. J. Biol. Macromol. 154 (2020) 104–113, https://doi.org/10.1016/j.ijbiomac.2020.02.330.

[20] Y. Cheng, H. Lin, Z. Chen, M. Megharaj, R. Naidu, Biodegradation of crystal violet using burkholderia vietnamiensis C09V immobilized on PVA–sodium alginate–kaolin gel beads, Ecotoxicol. Environ. Saf. 83 (2012) 108–114, https://doi.org/10.1016/j.ecoenv.2012.06.017.

[21] K.V. Kumar, Linear and non-linear regression analysis for the sorption kinetics of methylene blue onto activated carbon, J. Hazard. Mater. 137 (2006) 1538–1544, https://doi.org/10.1016/j.jhazmat.2006.04.036.

[22] M. Tanzifi, S.H. Hosseini, A.D. Kiadehi, M. Olazar, K. Karimipour, R. Rezaiemehr, I. Ali, Artificial neural network optimization for methyl orange adsorption onto polyaniline nano-adsorbent: kinetic, isotherm and thermodynamic studies, J. Mol. Liq. 244 (2017) 189–200, https://doi.org/10.1016/j.molliq.2017.08.122.

[23] M. Tanzifi, M.T. Yaraki, A.D. Kiadehi, S.H. Hosseini, M. Olazar, A.K. Bharti, S. Agarwal, V.K. Gupta, A. Kazemi, Adsorption of amido black 10B from aqueous solution using polyaniline/SiO2 nanocomposite: experimental investigation and artificial neural network modeling, J. Colloid Interface Sci. 510 (2018) 246–261, https://doi.org/10.1016/j.jcis.2017.09.055.

[24] John R. Koza, Genetic programming as a means for programming computers by natural selection, Stat. Comput. 4 (1994), https://doi.org/10.1007/BF00175355.

[25] S.H. Hosseini, M. Karami, H. Altzibar, M. Olazar, Prediction of pressure drop and minimum spouting velocity in draft tube conical spouted beds using genetic programming approach, Can. J. Chem. Eng. 98 (2020) 583–589, https://doi.org/10.1002/cjce.23590.

[26] F04 Committee Test Method for Determining the Chemical Composition and Sequence in Alginate by Proton Nuclear Magnetic Resonance (1H NMR) Spectroscopy ASTM International n.d. 10.1520/F2259-10R12E01.

[27] K. Haldar, S. Chakraborty, Investigation of chemical reaction during sodium alginate drop impact on calcium chloride film, Phys. Fluids 31 (2019), 072102, https://doi.org/10.1063/1.5100243.

[28] D.S. Cha, M.S. Chinnan, Biopolymer-based antimicrobial packaging: a review, Crit. Rev. Food Sci. Nutr. 44 (2004) 223–237, https://doi.org/10.1080/10408690490464276.

[29] M. Schmidt, H. Lipson, Distilling free-form natural Laws from experimental data, Science 324 (2009) 81–85, https://doi.org/10.1126/science.1165893.

[30] A.M. Ghaedi, A. Vafaei, Applications of artificial neural networks for adsorption removal of dyes from aqueous solution: a review, Adv. Colloid Interf. Sci. 245 (2017) 20–39, https://doi.org/10.1016/j.cis.2017.04.015.

[31] M.T. Hagan H.B. Demuth M.H. Beale O. De Jesus Neural network design 2nd edition Amazon Fulfillment Poland Sp. z o.o, Wroclaw, n.d.

[32] H. Qiu, L. Lv, B. Pan, Q. Zhang, W. Zhang, Q. Zhang, Critical review in adsorption kinetic models, J. Zhejiang Univ. Sci. A. 10 (2009) 716–724, https://doi.org/10.1631/jzus.A0820524.

[33] J.D. Seader, E.J. Henley, Separation Process Principles, 2nd ed, Wiley, Hoboken, N. J., 2006.

[34] Y.-C. Chang, D.-H. Chen, Adsorption kinetics and thermodynamics of acid dyes on a carboxymethylated chitosan-conjugated magnetic nano-adsorbent, Macromol. Biosci. 5 (2005) 254–261, https://doi.org/10.1002/mabi.200400153.

[35] X. Yang, B. Al-Duri, Kinetic modeling of liquid-phase adsorption of reactive dyes on activated carbon, J. Colloid Interface Sci. 287 (2005) 25–34, https://doi.org/10.1016/j.jcis.2005.01.093.

[36] J. Song, W. Zou, Y. Bian, F. Su, R. Han, Adsorption characteristics of methylene blue by peanut husk in batch and column modes, Desalination 265 (2011) 119–125, https://doi.org/10.1016/j.desal.2010.07.041.

[37] M.M.A. El-Latif M.F. El-Kady A.M. Ibrahim M.E. Ossman Alginate/ Polyvinyl Alcohol - Kaolin Composite for Removal of Methylene Blue from Aqueous Solution in a Batch Stirred Tank Reactor n.d. 13.

[38] G.N. Gubanova, V.A. Petrova, S.V. Kononova, E.N. Popova, V.E. Smirnova, A. N. Bugrov, V.V. Klechkovskaya, Y.A. Skorik, Thermal properties and structural features of multilayer films based on chitosan and anionic polysaccharides, Biomolecules. 11 (2021) 762, https://doi.org/10.3390/biom11050762.

[39] A. Tironi, M.A. Trezza, E.F. Irassar, A.N. Scian, Thermal treatment of kaolin: effect on the pozzolanic activity, Procedia Mater. Sci. 1 (2012) 343–350, https://doi.org/10.1016/j.mspro.2012.06.046.

[40] G. Lawrie, I. Keen, B. Drew, A. Chandler-Temple, L. Rintoul, P. Fredericks, L. Grøndahl, Interactions between alginate and chitosan biopolymers characterized using FTIR and XPS, Biomacromolecules 8 (2007) 2533–2541, https://doi.org/10.1021/bm070014y.

[41] M. Gorman, The evidence from infrared spectroscopy for hydrogen bonding: a case history of the correlation and interpretation of data, J. Chem. Educ. 34 (1957) 304, https://doi.org/10.1021/ed034p304.

[42] O.V. Ovchinnikov, A.V. Evtukhova, T.S. Kondratenko, M.S. Smirnov, V. Yu. Khokhlov, O.V. Erina, Manifestation of intermolecular interactions in FTIR spectra of methylene blue molecules, Vib. Spectrosc. 86 (2016) 181–189, https://doi.org/10.1016/j.vibspec.2016.06.016.

[43] B.J. Saikia, G. Parthasarathy, Fourier transform infrared spectroscopic characterization of kaolinite from Assam and Meghalaya Northeastern India, JMP 01 (2010) 206–210, https://doi.org/10.4236/jmp.2010.14031.

[44] M. Tanzifi, M. Tavakkoli Yaraki, M. Karami, S. Karimi, A. Dehghani Kiadehi, K. Karimipour, S. Wang, Modelling of dye adsorption from aqueous solution on polyaniline/carboxymethyl cellulose/TiO2 nanocomposites, J. Colloid Interface Sci. 519 (2018) 154–173, https://doi.org/10.1016/j.jcis.2018.02.059.

[45] A. Benhouria, Md.A. Islam, H. Zaghouane-Boudiaf, M. Boutahala, B.H. Hameed, Calcium alginate–bentonite–activated carbon composite beads as highly effective adsorbent for methylene blue, Chem. Eng. J. 270 (2015) 621–630, https://doi.org/10.1016/j.cej.2015.02.030.

[46] D. Ghosh, K.G. Bhattacharyya, Adsorption of methylene blue on kaolinite, Appl. Clay Sci. 20 (2002) 295–300, https://doi.org/10.1016/S0169-1317(01)00081-3.

[47] A.S. Eltaweil, G.S. Elgarhy, G.M. El-Subruiti, A.M. Omer, Carboxymethyl cellulose/carboxylated graphene oxide composite microbeads for efficient adsorption of cationic methylene blue dye, Int. J. Biol. Macromol. 154 (2020) 307–318, https://doi.org/10.1016/j.ijbiomac.2020.03.122.

[48] J. Fu, Zh. Chen, M. Wang, Sh. Liu, J. Zhang, J. Zhang, R. Han, Q. Xu, Adsorption of methylene blue by a high-efficiency adsorbent (polydopamine microspheres): Kinetics, isotherm, thermodynamics and mechanism analysis, Chem. Eng. J. (2015) 53–61, https://doi.org/10.1016/j.cej.2014.07.101.

[49] R. Pandimurugan, S. Thambidurai, Synthesis of seaweed-ZnO-PANI hybrid composite for adsorption of methylene blue dye, J. Environ. Chem. Eng. 4 (2016) 1332–1347, https://doi.org/10.1016/j.jece.2016.01.030.